Developing metabolomics for a systems biology approach to understand Parkinson's disease

Willacey, C.C.W.

Chapter 3

Metabolic profiling of material-limited cell samples by dimethylaminophenacyl bromide derivatization with UPLC-MS/MS analysis

Cornelius C W Willacey, Naama Karu, Amy C Harms and Thomas Hankemeier

Microchemical Journal (2020)
Volume 159, December 2020, 105445

Abstract

The ability to dissect the intracellular metabolome is vital in the study of diverse biological systems and models. However, limited cell availability is a challenge in metabolic profiling due to the low concentrations affecting the sensitivity. This is further exacerbated by modern technologies such as 3D microfluidic cell culture devices that provide a physiologically realistic environment, compared to traditional techniques such as cell culture in 2D well-plates. Attempts to address sensitivity issues have been made via advances in microscale separation such as CE and micro/nano-LC coupled to mass spectrometers with low-diameter ionization emitter sources. An alternative approach is sample derivatization, which improves the chromatographic separation, enhances the MS ionization, and promotes favourable fragmentation in terms of sensitivity and specificity. Although chemical derivatization is widely used for various applications, few derivatization methods allow sensitive analysis below 1×10^4 cells. Here, we conduct RPLC-MS/MS analysis of HepG2 cells ranging from 250 cells to 1×10^5 cells, after fast and accessible derivatization by dimethylaminophenacyl bromide (DmPABr), which labels the primary amine, secondary amine, thiol and carboxyl submetabolome, and also utilizes the isotope-coded derivatization (ICD). The analysis of 1×10^4 HepG2 cells accomplished quantification of 37 metabolites within 7-minute elution, and included amino acids, N-acetylated amino acids, acylcarntines, fatty acids and TCA cycle metabolites. The metabolic coverage includes commonly studied metabolites involved in the central carbon and energy-related metabolism, showing applicability in various applications and fields. The limit of detection of the method was below 20 nM for most amino acids, and sub 5 nM for the majority of N-acetylated amino acids and acylcarnitines. Good linearity was recorded for derivatized standards in a wide biological range representing expected metabolite levels in 2-10,000 cells. Intraday variability in 5×10^3 HepG2 cells was below 20% RSD for concentrations measured of all but two metabolites. The method sensitivity at the highest dilution of cell extract, 250 HepG2 cells, enabled the quantification of twelve metabolites and the detection of three additional metabolites below LLOQ. Where possible, performance parameters were compared to published methodologies that measure cell extract samples. The presented work shows a proof of concept for harnessing a derivatization method for sensitive analysis of material-limited biological samples. It

offers an attractive tool with further potential for enhanced performance when coupled to low-material suitable technologies such as CE-MS and micro/nano LC-MS.

Background

The study of the metabolome provides an important insight into biochemical processes within an organism in a range of environments. The field of metabolomics has been fast-evolving, and delivered quantitative and qualitative analysis of metabolites in various matrices from humans [1], animals [2], plants [3] and microbes [4], among others. Metabolomics analysis offers diagnostic support [5], and improves our understanding of disease mechanisms [6], therapeutic response [7] and off-target drug action [8]. Improvements in technology and knowledge create opportunities for new approaches to study intricate and dynamic biological systems, and many of these new approaches are the analysis of volume-limited samples and low concentration samples. Volume-limited and low concentration samples in metabolomics include microdialysate [9], CSF [10], microfluidic cell culture [11], region specific tissue sampling [12], blood and interstitial fluid collected by microneedle-arrays, and similar low-volume devices [13]. Metabolomics analysis of cells poses challenges due to the low availability of cell content, multiple analysis methods required in order to measure metabolites from different classes, and limited number of methods that offer accurate quantitation.

Over the past decade, 3D microfluidic cell cultures grew more popular as it provide a more realistic biological environment compared to conventional 2D culture techniques [14,15] and also offer high-throughput and dynamic sampling [14,16]. The majority of the devices used in microfluidic cell cultures are below 1×10^4 cell count, but not down to single-cell, as this represents a different field of study. Cell cultures are widely used for the research of various health conditions as they offer advantages in sample availability for multiple sets of experiments, fewer ethical considerations and more controlled conditions compared to limited clinical samples from patients. Unfortunately, the study of the intracellular metabolic profile is limited due to the aforementioned reasons, which are mainly low sensitivity and difficulty in the accurate quantitation of a wide range of relevant metabolites.

The metabolomics community tends to apply two analytical approaches in mass spectrometry to address volume/material-limited sample sensitivity issues. The most common approach is selection of advantageous technology and instruments to achieve the required application, and the less common approach is chemical derivatization to modify the analytes and improve the analysis performance [17]. The

former approach harnesses the advancements in technology by optimizing the separation technique, ionization interfaces or selecting the appropriate mass spectrometer design. Classic methods for the analysis of volume-limited samples use CE-MS [18], UPLC-MS [19], microLC-MS [20] and nanoLC-MS [21]. These techniques are often coupled to advanced ESI sources such as sheathless interfaces in CE [22,23] and micro-/nano-ESI emitters in LC-MS applications [21,24,25]. Despite miniaturized LC methods being available, a limited number of studies have used them to measure metabolites, and they are more common within the field of pharmacology and environmental sciences [26]. The latter approach, chemical derivatization, promotes sensitivity and accuracy in several ways: increased selectivity and resolution between interfering peaks (ion suppressors; isobaric and isomeric compounds); improved peak-shape; enhanced ionization efficiency, and more favorable ionization behaviour. Most derivatization reagents often increase the hydrophobicity of metabolites when the labelling group is relatively large (e.g. benzene rings) resulting in higher retention of metabolites on a reverse-phase column, requiring higher organic content in order to elute. The higher organic solvent content is more suitable for efficient ionization (i.e. improved desolvation), allowing more ions to enter the MS, thus promoting higher sensitivity [17]. Chemical derivatization has been instrumental in GC-MS for several decades to improve volatility, separation and sensitivity [27], and there has been a recent resurgence in modern analytical applications using non-GC methods. Chemical derivatization strategies such as benzoyl chloride [28], dansyl chloride [29], dimethylaminophenacyl bromide (DmPABr) [30] and N-dimethyl-amino naphthalene-1-sulfonyl chloride (Dns-Cl) [31] are commonly referenced and applied to label specific functional groups. Recently, Lkhagya *et al.* compared the sensitivity gain that can be achieved in LC-MS/MS by different derivatization reagents, Dansyl, OPA, Fmoc, Dabsyl and Marfey's, when applied to metabolically characterize a medicinal Chinese herb [32]. They showed that each reagent has its own strength in producing a sensitivity gain, and the main limitation was metabolome coverage. The derivatization strategies mentioned above also employ the isotope-coded derivatization (ICD) approach [17] in which the metabolites of interest are labelled by both a derivatization reagent and an isotopically-labelled reagent, generating an internal standard for each metabolite, with full coverage and in a cost-effective manner. While most publications of methods that target volume/material-limited samples discuss the sensitivity enhancements achieved via introduction of the chemical label, only a few

publications offer methodical evaluation of the sensitivity gain over conventional approaches [28,29,33]. Despite its advantages, derivatization techniques suffer from some limitations. They involve time-consuming processes, require additional processing steps (risk of errors), and depend on labelling efficiency (reproducibility of recovery), which also limits the coverage according to the reagent reactivity with the functional groups. Fortunately, chemical reagents have been developed to cover the majority of functional groups found within the human metabolome. The reagents benzoyl chloride, dansyl chloride and Dns-Cl label metabolites containing amine, phenol and thiol functional groups.

In a recent publication, we demonstrated a method that expands the functional group coverage of DmPABr to label primary amines (twice), secondary amines (once), thiols (once) and carboxylic acids (once) (derivatization reaction shown in Fig 3.1), further enhancing the quantitative coverage of the human metabolome [34]. However, we intentionally reduced the ionization and collision energy efficiency to allow quantitation, within the dynamic range of the detector, of high abundance metabolites in urine and cells in high numbers. In the presented work, we show a proof-of-concept for the analysis of cells in the microfluidic range (below 1×10^4 cells) following derivatization with the reagent DmPABr. Additionally, we evaluate the performance of the targeted quantitative method applying the DmPABr reagent against commonly utilised methods. We demonstrate absolute quantification of the central carbon and energy metabolism in a low cell-count sample of human HepG2 cells, which are commonly used to demonstrate analytical methods due to their robustness and ease of use. Two million HepG2 cells were lysed and further diluted to solutions containing 1×10^5 to 250 cells, representing the microfluidic cell culture range. Cell dilution is a common approach, however, it does not address additional limitations in microfluidic cell culture devices, mainly discrepancies in metabolite concentrations per cell number extract, as stated by Gunda *et al.* [35]. With regards to metabolic coverage, we selected the metabolites due to their wide range of physicochemical properties, ability to be derivatized by DmPABr, applicability to human diseases, and coverage by other previously-published volume-limited sample analyses, in order to provide a fair comparison. The metabolites covered within this method include amino acids, N-acetylated amino acids, acylcarnitines and organic acids. We showcase the capability of the DmPABr derivatization method to provide a

sensitive quantitative analysis of low numbers of HepG2 cells without the need for miniaturised separation and ionization techniques.

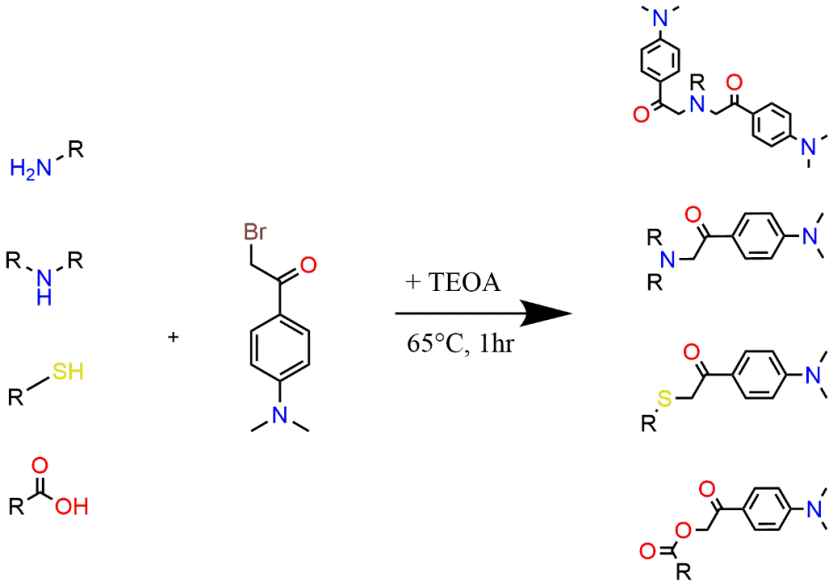

Fig 3.1. The derivatization reaction of DmPABr with the primary amine, secondary amine, thiol and carboxylic acid, respectively.

Materials and Methods

Chemicals

All chemicals were purchased from Sigma-Aldrich (St. Louis, USA) unless stated otherwise. Stock solutions of 5 mg/mL L-alanine (Ala), L-arginine (Arg), L-asparagine (Asn), L-aspartic acid (Asp), L-cysteine (Cys), L-glutamine (Gln), L-glutamic acid (Glu), glycine (Gly), L-histidine (His), L-isoleucine (Ile), L-leucine (Leu), L-lysine (Lys), L-methionine (Met), L-phenylalanine (Phe), L-proline (Pro), L-serine (Ser), L-threonine (Thr), L-tryptophan (Trp), L-tyrosine (Tyr), L-valine (Val) and creatinine (CR) were solubilized in DMSO/DMF (1:1 v/v) and were stored at -80 °C. Additionally, 1 mg/mL N-acetylalanine (NA-Ala), N-acetylarginine (NA-Arg), N-acetylaspartic acid (NA-Asp), N-acetylglutamine (NA-Gln), N-acetylglycine (NA-Gly), N-acetylmethionine (NA-Met), N-acetylthreonine (NA-Thr), N-acetyltryptophan (NA-Trp), N-acetyltyrosine (NA-Tyr), N-acetylvaline (NA-Val), α-ketoglutaric acid (AKG), citric/isocitric acid (CITS), fumaric acid (FUM), lactic acid (LAC), malic acid (MAL), oxaloacetic acid (OXA), pyruvic acid (PYR), succinic acid (SUCC), acetylcarnitine (C2:0-carnitine), decanoylcarnitine (C10:0-carnitine), hexanoylcarnitine (C6:0-carnitine), lauroylcarnitine (C12:0-carnitine), myristoylcarnitine (C14:0-carnitine), octanoylcarnitine (C8:0-carnitine), palmitoylcarnitine (C16:0-carnitine), propionylcarnitine (C3:0-carnitine) and stearoylcarnitine (C18:0-carnitine) were solubilized in DMSO/DMF (1:1 v/v) and stored at −80 °C. Undecanoic acid (C11:0), dodecanoic acid (C12:0), octanoic acid (C8:0) and decanoic acid (C10:0) were solubilized at 1 mg/mL in ACN. The LC-MS grade ACN, DMSO and DMF were sourced from Actu-all Chemicals (Oss, The Netherlands). Dimethylaminophenacyl bromide (DmPABr) was procured from BioConnect BV (Huissen, The Netherlands) and DmPABr-$^{13}C_2$ was purchased from Nova Medical Testing (Alberta, Canada). In addition, the list of chemical identifiers (ChEBI IDs) can be found in supplementary Table S1.

HepG2 sample collection and preparation

The HepG2 cells were seeded and cultured at 37 °C under 5 % CO_2, harvested after 5 days and rinsed with PBS at 37 °C. The HepG2 cells were then separated into Eppendorf vials containing 2×10^6 cells per vial, and stored at -80 °C until sample preparation. Sample preparation consisted of reconstitution immediately in 1 mL of

water/methanol (1:4 v/v), followed by 5 minutes of sonication and vortexing to lyse the cells. The cells were then centrifuged at 13,000 rpm for 10 minutes at 4 °C to allow protein precipitation using an Eppendorf 5427R Centrifuge (Hamburg, Germany). The supernatant was transferred to a new Eppendorf vial and further diluted using water/methanol (1:1 v/v) to the equivalent cell contents of 1×10^5, 5×10^4, 2.5×10^4, 1×10^4, 5×10^3, 2.5×10^3 and 1×10^3, 500 and 250.

Derivatization of HepG2 cells

Triplicates of HepG2 cell supernatant containing the equivalent cell volume ranging from 250 to 1×10^5 were dried in a Labconco SpeedVac (MO, United States). Each dried sample was reconstituted immediately in 10 µL of DMSO/DMF (1:1 v/v) to dissolve both polar and apolar metabolites, followed by the addition of 10 µL triethanolamine (750 mM) and 20 µL DmPABr (40 mg/mL). The content was then kept at 65 °C for 1 hour, followed by the addition of 10 µL formic acid (30 mg/mL), and further 30 minutes at 65 °C to quench the reaction. After this, 5 µL of DmPA-$^{13}C_2$ labelled metabolite internal standard and 45 µL acetonitrile were added, bringing the total volume up to 100 µL. The stability of DmPABr derivatized samples were demonstrated previously [30].

Chromatography conditions

The LC method conditions were detailed previously [34] with further adaptations. The method modifications focused on the retention times of the internals standards as the DmPA-D_6 was changed to DmPA-$^{13}C_2$ resulting in co-elution with each metabolite. The target metabolites were separated using a Waters Acquity UPLC Class II (Milford, USA) on an AccQ-tag C18 column [2.1 x 100 mm, 1.4 µm (Milford, USA)] kept at 60 °C, using gradient elution at a flow rate of 0.7 mL/min. Mobile phase A consisted of water containing 10 mM ammonium formate and 0.1% formic acid, and mobile phase B was 100% acetonitrile. The gradient profile was as follows; starting at 0.2 % B; linear increase to 20 % B at 1.5 min, 50 % B at 4.0 min, 90 % B at 6.0 min, 99.8 % B at 10.0 min and maintained until 13.0 min, then back to start conditions at 13.1 min, equilibrating until 15.0 min. The flow of the first 1.2 minutes was diverted to waste to prevent the DMSO/DMF peak from entering the mass spectrometer. The autosampler was maintained at 10 °C, and the injection volume was 1 µL.

Mass spectrometry and data generation

An AB Sciex QTrap 6500 mass spectrometer (Framingham, USA) was operated in positive ionization mode to accommodate the tertiary amine introduced by the derivatization reagent. The MS parameters were set as follows: curtain gas - 30.0 psi; collision gas - medium; ionization voltage - 5500 V; temperature - 600°C; ion source gas 1 at 60.0 psi; ion source gas 2 at 50.0 psi.

MRM optimization was achieved per analyte by independently derivatizing each analyte and then conducting direct infusion in compound optimization analysis mode. The MRM channels were optimized for entrance potential, declustering potential and exit potential. For each analyte, a unique fragmentation pattern was favoured, and the most abundant product ion was selected to provide the optimal sensitivity. The full details of the DmPABr derivatized metabolites, MRM parameters, and MS conditions can be found in supplementary Table S2.

The data was integrated using the AB Sciex MultiQuant Workstation Quantitative Analysis for QTrap. Automatic integration was used where possible and with a manual visual inspection conducted to ensure reliable integration. The data was assessed using peak area ratios ($P_{analyte}/P_{Internal\ standard}$). For statistical analysis, Microsoft Excel and GraphPad Prism 8 (La Jolla, CA) was used. We assessed the method using four independently made matrix-free calibration lines. We conducted a calibration concentration starting at the same concentration listed in supplementary Table S3, and diluted by 2-fold until the LOD was reached for both methods. Additionally, we used the equivalent of 5×10^3 cells (n = 3) to assess the intraday variability of the method. All concentrations reported represent the intracellular concentration of the extracted HepG2 cells. The LOD and LOQ were calculated using the following equations using the ICH Q2 guidelines (σ = standard deviation of the lowest calibration point):

$$LOD = (3.3 * \sigma) / slope$$

$$LOQ = (10 * \sigma) / slope$$

Results & Discussion

Separation profile advantages of derivatization

Derivatization with DmPABr prior to RPLC offers advantages in the separation profile of the targeted metabolites, that otherwise may co-elute, or elute early

alongside some high-abundance compounds which may act as ion suppressors. Other analytical techniques, such as CE-MS, may exhibit similar separation issues during sensitive analysis of cells [22]. In addition, compromised peak-shape is an issue that often arises during the separation of amino acids [36] and organic acids on a HILIC column [37]. HILIC methods have been established that measure amino acids, organic acids [38] and acylcarntines [39] with good peak-shape, yet they usually require longer acquisition time, and they do not offer universal coverage within one injection because both positive and negative ionisation mode are required.

Figure 3.2 presents the chromatograms of the different MRM channels for amino acids measured quantitatively in 5×10^3 HepG2 cell extracts. Following derivatization, the chromatogram shows ideal peak shape of amino acids that usually suffer from early elution and poor peak-shape on RPLC. Moreover, isomeric metabolites such as leucine and isoleucine can be baseline resolved (see supplementary figure S2). The peak width at half height measured for alanine, N-acetylaspartic acid, leucine and isoleucine was 1.071, 1.001, 0.943 and 0.909 seconds, respectively. This demonstrates that derivatization with DmPABr followed by RPLC can compete with CE in terms of peak width. However, sharp peaks also require suitable mass spectrometers to record a sufficient number of data points across a peak, using small scan times. Processing large batches of samples using small time windows can be challenging due to retention shifts. Fortunately, the retention time repeatability of this method was high for all metabolites, for example, the retention time relative standard deviation for alanine, N-acetylaspartic acid and myristoylcarnitine was 0.014 %, 0.016 %, 0.034 %, respectively, in three measurements of 1×10^4 HepG2 cells extracts along 22.5 hours. In comparison, separation techniques such as CE may experience migration time RSD between 2% and 3% [22]. Using HILIC separation, the analysis of apolar metabolites and organic acids have posed challenges due to non-Gaussian peak shape. Fig 3.3 demonstrates how derivatization provides greater retention and improved peaks shapes for such problematic organic acids, including lactic acid (monocarboxylic acid), oxaloacetic acid (ketoacid) and succinic acid (dicarboxylic acid). In addition, aromatic amino acids and acylcarnitines also suffer from poor peak shape on HILIC, yet after derivatization they behave more favourably on RPLC. Another peak shape parameter assessed here was the asymmetry, which generally showed very good results. For example, in neat calibration solution, the asymmetry factor of phenylalanine, tryptophan, lactic acid, succinic acid,

palmitoylcarnitine and steroylcarnitine was 0.91, 1.19, 0.98, 1.15, 1.06 and 1.10, respectively (additional asymmetry factors for neat standards are shown in supplementary Table S5).

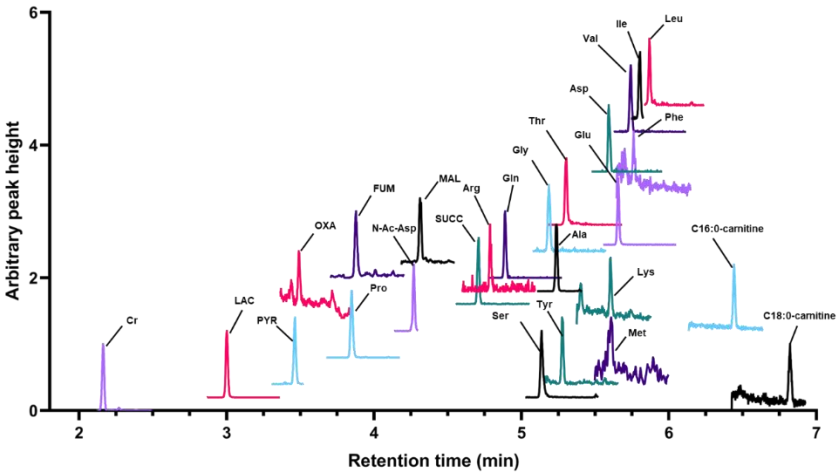

Fig 3.2. LC-MS/MS analysis of 5×10³ HepG2 cells shown in multi-reaction monitoring (MRM) in positive ionisation mode after derivatization with DmPABr. Only the metabolites above the LOQ are shown in this chromatogram. The peak intensity of each signal was scaled to a uniform height and does not represent actual peak height.

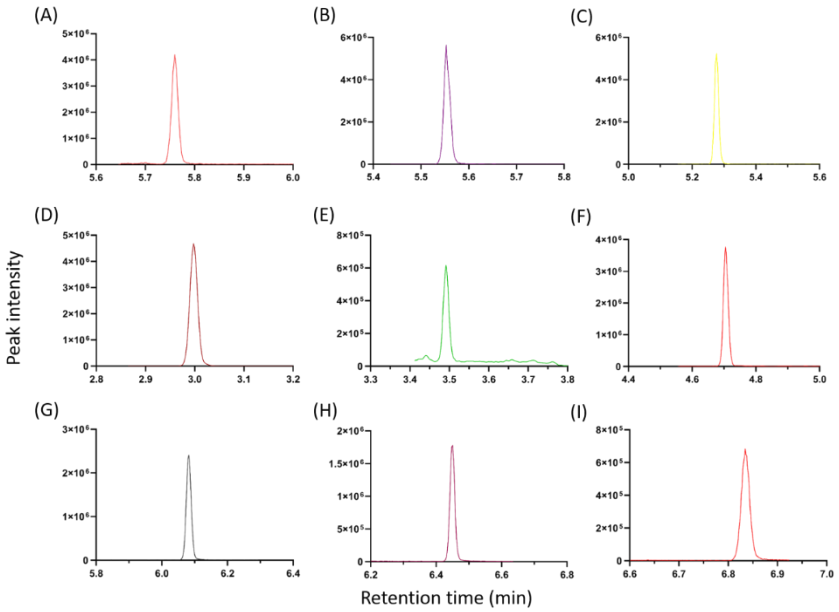

Fig 3.3. The extracted ion chromatogram of the derivatized metabolites measured in matrix-free solution showing the midpoint calibration concentration (supplementary Table S3). The metabolites shown are phenylalanine (A), tryptophan (B), tyrosine (C), lactic acid (D), oxaloacetic acid (E), succinic acid (F), palmitoylcarnitine (G), myristoylcarnitine (H) and steroylcarnitine (I). The specific MRM transitions are given in supplementary Table S2.

Method performance in matrix-free standard solutions

The general performance of the DmPABr method was already evaluated in previous work [34]. Here, we demonstrate the method suitability for metabolomics analysis of HepG2 cells, which requires tailored optimisation and modified calibration ranges. The performance parameters summarized in Table 3.1 are the linear range, coefficient of determination and repeatability expressed as the relative standard deviation of quadruplets of the middle calibration point. The linearity of the majority of metabolites in the low concentration range were above R^2 of 0.990, except for asparagine, glutamic acid, phenylalanine, tryptophan, N-Ac-methionine, oxaloacetic acid and dodecanoic acid, but they were deemed to be within an acceptable range for

consideration. Interestingly, the metabolites with an R^2 <0.990 belong to a range of chemical classes with a range of physiochemical properties, further supporting our earlier observation that the variability is not due to derivatization efficiency of specific functional groups [34]. Furthermore, the lower concentration ranges (sub 250 nM) are prone to higher variability which may explain the compromise in linearity. Overall, the method exhibited good repeatability (n = 4) at the middle calibration point which represents an estimate of 5×10^3 HepG2 cells. The RSD was below 20 % for all metabolites measured in neat solutions by the method, providing consistent quantitative results. For example, metabolites such as alanine, lactic acid and lauroylcarnitine had an RSD of 2.6 %, 0.8 % and 1.2 %, respectively, demonstrating the low variability in different functional groups including primary amine, carboxylic acid and quaternary amine.

Metabolite	Linear range (nM)	R^2	RSD (%)	Metabolite	Linear range (nM)	R^2	RSD (%)
Alanine	70-1060	0.998	2.6	**N-acetylthreonine**	2-1250	0.999	14.7
Arginine	10-600	0.994	16.8	**N-acetyltryptophan**	5-450	0.997	13.3
Asparagine	60-530	0.988	3.7	**N-acetyltyrosine**	0.5-250	0.998	4.2
Aspartic acid	80-700	0.993	16.3	**N-acetylvaline**	5-1100	0.997	11
Cysteine	400-7000	0.995	14.8	**α-Ketoglutaric acid**	20-1400	0.994	8.3
Glutamine	50-1700	0.991	11.5	**Citrates**	450-30000	0.993	7.7
Glutamic acid	60-2350	0.984	5.1	**Fumaric acid**	60-1900	0.987	5.8
Glycine	500-60000	0.999	7	**Lactic acid**	500-20000	0.999	0.8
Histidine	900-14000	0.991	12.1	**Malic acid**	5-950	0.998	9
Isoleucine	10-250	0.995	9.6	**Oxaloacetic acid**	30-1900	0.989	5.7
Leucine	10-350	0.995	3.8	**Pyruvic acid**	20-1400	0.995	1.3
Lysine	500-7000	0.991	3.3	**Succinic acid**	50-1900	0.997	2.7
Methionine	30-950	0.998	6	**Acetylcarnitine**	30-1900	0.997	15.7
Phenylalanine	40-700	0.984	4.7	**Decanoylcarnitine**	1-1800	1	4.2
Proline	60-1900	0.999	3.7	**Hexanoylcarnitine**	10-1800	0.999	8.2
Serine	100-3500	0.99	10	**Lauroylcarnitine**	1-1800	0.999	1.2
Threonine	20-700	0.99	12.2	**Myristoylcarnitine**	5-1800	0.999	4.6
Tryptophan	40-700	0.985	10.1	**Octanoylcarnitine**	5-190	0.999	8.6

Metabolite	Linear range (nM)	R^2	RSD (%)	Metabolite	Linear range (nM)	R^2	RSD (%)
Tyrosine	60-950	0.994	3	**Palmitoylcarnitine**	5-1800	0.999	5.9
Valine	30-500	0.991	3.6	**Propionylcarnitine**	5-1800	0.999	1.9
N-acetylalanine	5-1250	0.999	2.4	**Stearoylcarnitine**	5-1800	1	3
N-acetylarginine	0.5-1100	1	11.5	**Decanoic acid**	5-1900	0.997	1.7
N-acetylaspartic acid	1-750	0.992	12.1	**Octanoic acid**	30-3700	0.997	5.1
N-acetylglutamine	5-1150	0.997	3.5	**Dodecanoic acid**	120-900	0.98	8.6
N-acetylglycine	1-600	0.998	15.1	**Undecanoic Acid**	5-750	0.994	6.5
N-acetylmethionine	2-1450	0.988	15.4	**Creatinine**	50-7000	1	7

Table 3.1. Summary of the method performance showing the linear range, linearity and RSD of the method in neat solution. The RSD was assessed at the midpoint concentration of the low concentration calibration line.

Method performance across varying dilutions of HepG2 cells

To address the needs of microfluidics cells analysis, where good performance is required below 1×10^4 cells, the quantitative metabolic coverage was measured in cellular extracts equivalent to the cellular content of 250 to 1×10^5 HepG2 cells. Table 3.2 presents the metabolites that could be quantified and detected (below LLOQ) across a range of cell extract dilutions, ranging from 1×10^5 cells extract down to dilution containing 250 cells (equivalent to less than a cell loaded on the column). All of the amino acids, except histidine, were detected below 1×10^4 cells. Histidine is the only metabolite within this method that is double charged, making the metabolite more vulnerable to in-source fragmentation, thus reducing the sensitivity in limited MRM setup. Additionally, 13 amino acids were quantified in 1×10^3 HepG2 cells, and alanine, glutamic acid, glycine, proline, serine, threonine and valine were quantified in 250 cells. Unlike amino acids, the majority of N-acetylated amino acids exist in relatively low concentrations within the cells. Nevertheless, 8 out of 14 metabolites included in the method were successfully detected in the 1×10^4 cells extract, and the mitochondria active N-acetylaspartic acid could be detected in 250 HepG2 cells. N-acetylated amino acids can be found in high concentrations in the extracellular environment, which is an interesting direction to further investigate the applicability

of the current method in low cell numbers [40]. The 9 acylcarnitines targeted in this method were quantified in 5×10^4 cells, and four in 1×10^4 cells. Additionally, all acyl carnitines (except acetylcarnitine) could be detected in 1×10^4 cells. The method also covers organic acids and, as mentioned previously, the main strength of DmPA-labelling of organic acids is achieved by the addition of a tertiary amine, resulting in higher sensitivity despite susceptibility of the unlabelled metabolite to ion suppression in the ESI source [41]. TCA cycle intermediates were detected with very good sensitivity. α-ketoglutarate, citrates, malic acid, oxaloacetic acid and pyruvic acid were detected in 1×10^4 cells, and fumaric acid, malic acid and pyruvic acid were further quantified in 250 cells. The quantified concentrations of these metabolites agrees with previously published data showing that within the TCA cycle, α-ketoglutarate and oxaloacetic acid are present at lower concentrations, hence are more challenging to quantify [34]. The quantitation of energy and central carbon-related metabolites can improve our understanding of the health and functionality of cells, and applying this to 3D microfluidic cells provides an accurate and true recording of the physiological environment.

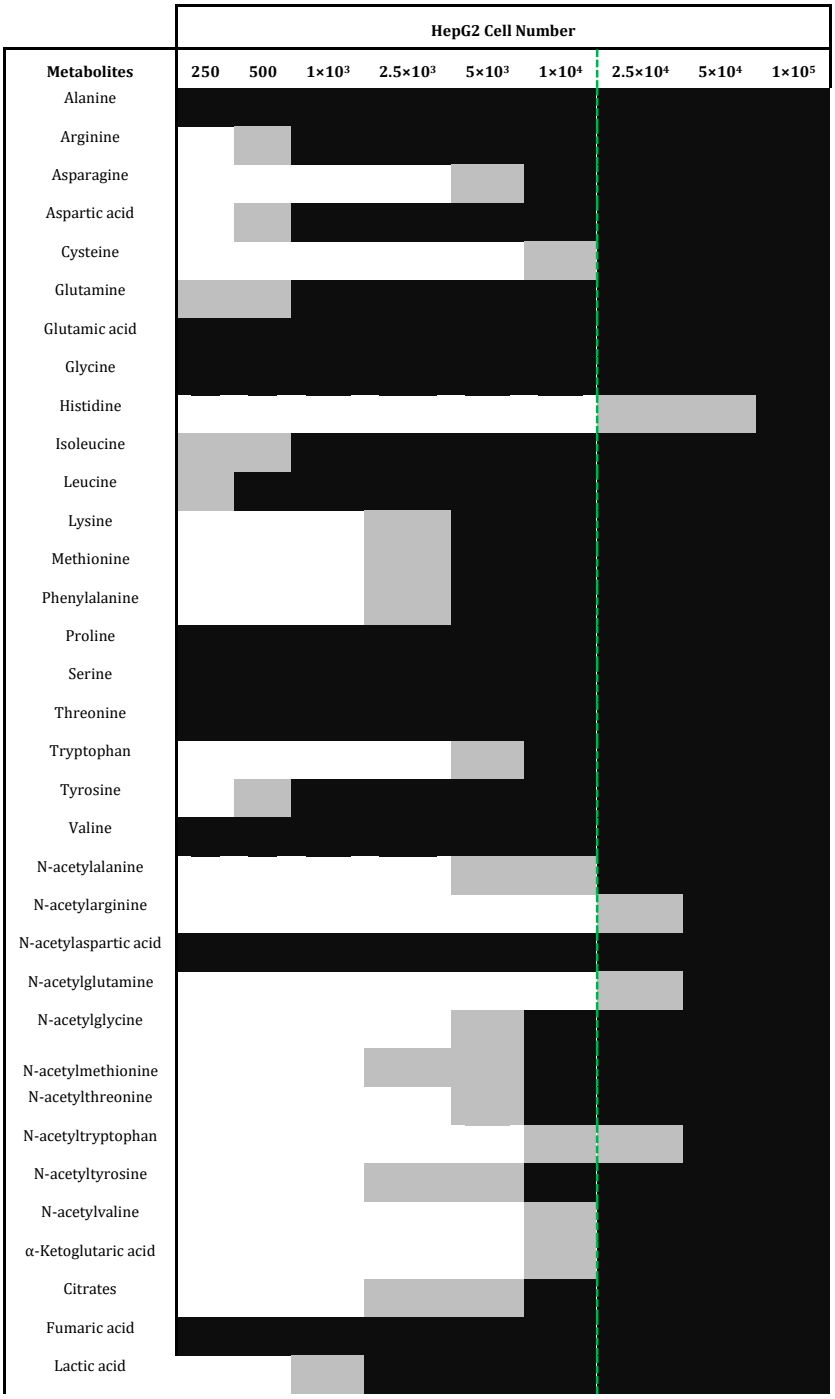
HepG2 Cell Number
Metabolites
250
500
1×10³
2.5×10³
5×10³
1×10⁴
2.5×10⁴
5×10⁴
1×10⁵
Alanine
Arginine
Asparagine
Aspartic acid
Cysteine
Glutamine
Glutamic acid
Glycine
Histidine
Isoleucine
Leucine
Lysine
Methionine
Phenylalanine
Proline
Serine
Threonine
Tryptophan
Tyrosine
Valine
N-acetylalanine
N-acetylarginine
N-acetylaspartic acid
N-acetylglutamine
N-acetylglycine
N-acetylmethionine
N-acetylthreonine
N-acetyltryptophan
N-acetyltyrosine
N-acetylvaline
α-Ketoglutaric acid
Citrates
Fumaric acid
Lactic acid

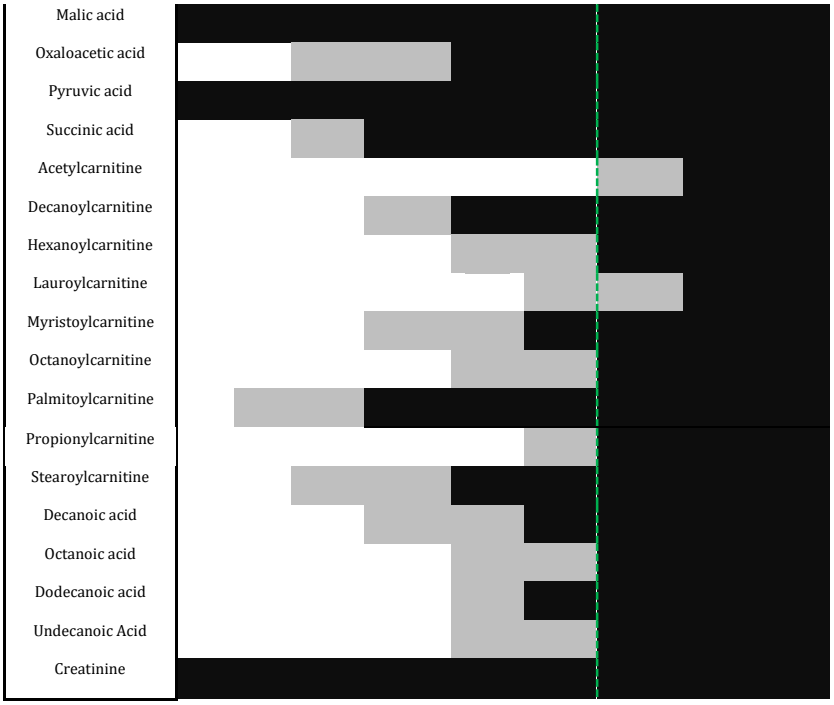

Table 3.2. Detection and quantitation of metabolites by the DmPABr derivatization method, applied to a range of HepG2 cell numbers (250-1×10^5). The shaded cells represents the detection in that dilution of cells: Black, >LLOQ; Grey, <LLOQ and >LOD; white, <LOD. The dotted green line shows the different cells number zones of microfluidic cell culture number (left of line) and macroscopic cell culture (right of line).

Table 3.2 demonstrates that the method can quantitatively analyze a range of metabolites with varying functional groups and physicochemical properties in the range of HepG2 cell counts. The linearity of calculated concentration along the range of cell dilutions is depicted for selected metabolites in Fig 3.4, and further detailed in supplementary Table S4. These plots visualise the applicability of DmPABr derivatization to microfluidic cell culture ranges which are sub-1×10^4 cells. Generally, good linearity is observed throughout the range of cell dilutions, apart from specific cases where linearity was limited for the lower range of cell count. This behaviour is not unexpected due to solvation and ionisation efficiency and still aligns well the aim of the work. This effect is also observed in supplementary figure S1 that

shows the total ion chromatograms of the MRM channels recorded when the method was applied on 3 different cell dilutions.

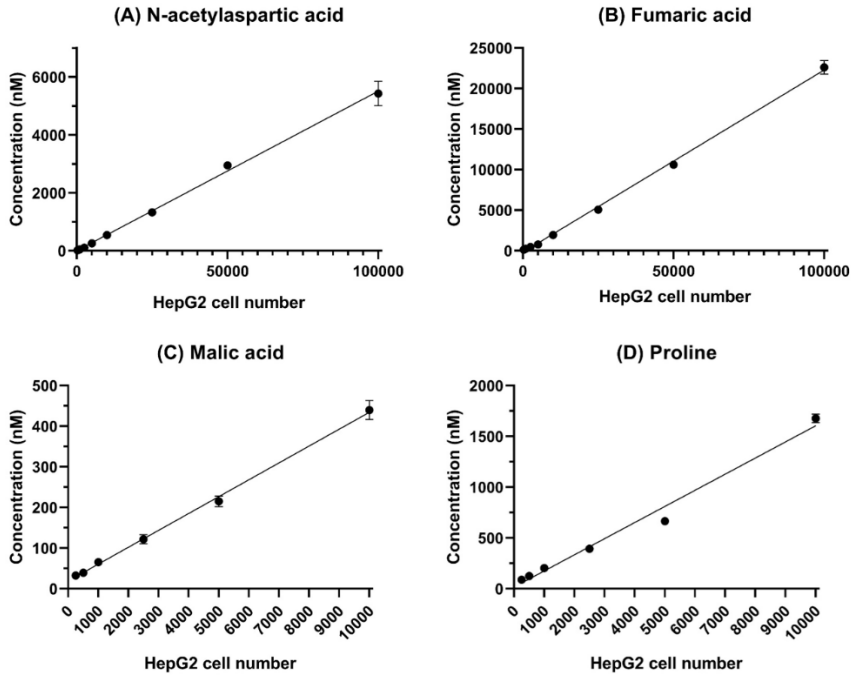

Fig 3.4. Quantification of selected metabolites in a range of cell counts. A) N-acetylaspartic acid and B) fumaric acid measured in 250 to 1×10^5 HepG2 cells (n = 3); C) malic acid and D) proline measured in 250 to 1×10^4 HepG2 cells (n = 3).

Quantitative results in 5000 HepG2 cell extract

The DmPABr LC-MS/MS method presented here was adapted from our previously published method [34], by optimizing the MRM parameters and increasing ionisation voltages, to increase the sensitivity across the metabolites range. Table 3.3 summarizes the absolute quantitation of central carbon and energy-related metabolites in 5×10^3 HepG2 cell extracts (equivalent of 5 cells on column) by employing the ICD approach using DmPA-$^{13}C_2$–labelled metabolites as a corresponding internal standard. Amino acids such as arginine and phenylalanine can be quantified despite low abundance (41.0 and 88.5 nM, respectively). The

mitochondrial abundant metabolite N-acetyl aspartate, which is associated with several diseases including Parkinson's disease, Canavan disease and Leigh's syndrome, was quantified at 261.6 nM. However, other N-acetylated amino acids, such as N-acetylglycine, N-acetylmethonine and N-acetylthreonine, were detected below the LLOQ. TCA cycle intermediates and pyruvic acid were also captured by the method at these cell number ranges, which could further support the study of energy metabolism within low cell numbers in a physiological-presenting environment using 3D microfluidic cell culture. After optimisation of the ionization voltage and collision energy from the previously published method, the LOD of metabolites such as serine improved from 506 nM to 23.4 nM, glycine from 932.4 to 25.7 nM, and N-acetylthreonine from 10.4 to 2.2 nM. Similarly, the LOD of α-ketoglutarate decreased from 29.7 down to 15.6 nM [34]. The majority of late eluters showed the most sensitivity gain compared to early eluters, probably due to improved desolvation conditions owing to higher organic solvents, as discussed previously. The asymmetry factor during the measurement of 5×10^3 HepG2 cell extract for alanine, N-acetylaspartic acid, glutamine, leucine, isoleucine, succinic acid and malic acid was 0.96, 0.95, 0.96, 1.00, 1.13, 0.88 and 0.94, respectively, demonstrating a close-to-Gaussian profile, without a specific tendency for tailing or fronting. The variability of the 5×10^3 HepG2 cells measurements observed for almost all metabolites was well below RSD of 20%. Higher RSD values were recorded for decanoylcarnitine and hexanoylcarnitine (34.5 % and 66 %, respectively), probably due to the increased background noise (as discussed previously). Nonetheless, we chose to include and present this data to identify required improvements that may further increase the sensitivity and repeatability. These metabolites could warrant the use of MS^3 which provides the ability to reduce background noise and increase sensitivity [42].

Metabolite	Conc. (nM)	LOD (nM)	Asymmetry factor	RSD (%)	Metabolite	Conc. (nM)	LOD (nM)	Asymmetry factor	RSD (%)
Alanine	666	14.9	0.96	2.1	**N-acetylthreonine**	<LOQ	2.2	0.86	19.1
Arginine	41	2.9	0.74	10.4	**N-acetyltryptophan**	ND	8.3	N/A	N/A
Asparagine	<LOQ	43.4	1.59	3.4	**N-acetyltyrosine**	<LOQ	0.2	1.91	14.8
Aspartic acid	595.4	57.4	1.33	11.9	**N-acetylvaline**	ND	0.7	N/A	N/A
Cysteine	ND	366.4	N/A	N/A	**α-Ketoglutaric acid**	ND	15.6	N/A	N/A
Glutamine	285.8	32.8	0.96	6.3	**Citrates**	<LOQ	181.4	4.02	3
Glutamic acid	2138.7	39.6	1.39	9.1	**Fumaric acid**	774.3	9.3	2.32	5
Glycine	1404.1	25.7	1.48	0.8	**Lactic acid**	662.5	70.5	0.90	4.9
Histidine	ND	803.7	N/A	N/A	**Malic acid**	215.2	5.5	0.94	6
Isoleucine	56.9	4.2	1.13	5.2	**Oxaloacetic acid**	82.5	10.3	1.14	2.6
Leucine	95	4.8	1.00	7.5	**Pyruvic acid**	309.3	11.5	0.92	3.9
Lysine	553	17.9	1.41	0.4	**Succinic acid**	253.2	21.7	0.88	2.5
Methionine	85.6	3.8	0.82	16.2	**Acetylcarnitine**	ND	21.1	ND	N/A
Phenylalanine	88.5	3.7	2.47	7.5	**Decanoylcarnitine**	4.1	0.7	3.08	34.5
Proline	666.6	7.4	1.32	3.6	**Hexanoylcarnitine**	<LOQ	4.2	1.80	66
Serine	704	23.4	2.06	2.6	**Lauroylcarnitine**	ND	1	ND	N/A
Threonine	348.8	11.7	1.72	5.1	**Myristoylcarnitine**	<LOQ	2.4	1.00	11.1
Tryptophan	<LOQ	26.7	0.63	1.2	**Octanoylcarnitine**	<LOQ	2.8	0.60	12.7
Tyrosine	114.3	9.7	0.86	5.6	**Palmitoylcarnitine**	4.9	0.2	0.79	14.9
Valine	108	12.4	0.93	6.1	**Propionylcarnitine**	ND	3.6	N/A	N/A
N-acetylalanine	<LOQ	6.8	1.01	5.2	**Stearoylcarnitine**	4.4	3.6	1.53	15.3
N-acetylarginine	ND	1.4	N/A	N/A	**Decanoic acid**	<LOQ	1.4	0.94	2.5
N-acetylaspartic acid	261.6	1.1	0.95	9	**Octanoic acid**	<LOQ	25	0.95	10.8
N-acetylglutamine	ND	3.9	N/A	N/A	**Dodecanoic acid**	<LOQ	80.7	1.14	10.6
N-acetylglycine	<LOQ	2.1	0.64	14.5	**Undecanoic Acid**	<LOQ	3.8	1.11	6
N-acetylmethionine	<LOQ	0.9	1.83	12.3	**Creatinine**	2167.7	36.8	0.83	9.8

Table 3.3. Method performance of derivatized metabolites in the analysis of 5×10^3 HepG2 cells. Repeatability is expressed as %RSD of concentration for sample measured in triplicate intraday from different samples; <LOQ, the metabolite was detected but falls below the low limit of quantitation; ND, the metabolite was not detected in an extract from 5×10^3 cells; N/A, not applicable.

Sensitivity compared to commonly used methods

Several chromatographic techniques have been applied in the pursuit of sensitive metabolite analysis of volume-limited samples. The use of HILIC-MS is a common approach for measuring amino acids and organic acids from cell lysate. Liu *et al.* [43] quantified 107 metabolites in Huh-7 cells with the use of 10 internal standards in a 25-minute HILIC-MS/MS method. The method achieved amino acids LODs of 30 nM for phenylalanine (vs. 3.7 nM by DmPABr), 1000 nM for tryptophan (vs. 26.7 nm with DmPABr), 3000 nM for glycine (vs. 25.7 nM for DmPABr). Additionally, organic acids had a LODs of 330 nM for alpha-ketoglutarate (vs. 15.6 nM for DmPABr), 200 nM for succinic acid (vs. 21.7 nM for DmPABr), and 250 nM for malic acid (vs. 5.5 nM for DmPABr). This shows a significant increase in sensitivity compared to HILIC-MS/MS methods and a reduced analysis time. In a recent work by Zhang *et al.* [22], sheathless CE-MS enabled the detection of amine-containing metabolites down to 500 HepG2 cell extracts. This method achieved LODs of 4.5 nM for alanine (vs. 14.9 nM by DmPaBr), 1.0 nM for glutamic acid (vs. 39.6 nM by DmPaBr), 5.7 nM for glutamine (vs. 32.8 nM by DmPaBr), 7.9 nM for tryptophan (vs. 26.7 nM by DmPaBr), and 2.9 nM for valine (vs. 12.4 nM by DmPaBr). This demonstrates that sheathless CE-MS is more sensitive to amino acids than DmPABr, however it requires an advanced separation technology that is less robust than RPLC, has less universal coverage of the metabolome, and the lack of internal standard coverage reduces quantitative performance. Additionally, it should be noted that different calculations were used to obtain the LOD, and the sheathless CE approach used signal-to-noise extrapolation. The sheathless CE-MS approach also struggles with the separation and sensitive detection of organic acids due to the lack of positively ionisable groups. This is another advantage that DmPA-labelling achieves by introducing a tertiary amine onto organic acids, thus enabling sensitive detection in positive ionisation mode (for example, malic acid and pyruvate at 5.5 nM and 11.5 nM LOD, respectively). GC-MS is another approach utilized to measure amino acids and organic acids from cell lysate, yet it can be compromised by lower sensitivity. The method applied by Danielsson *et al.* [44] provides varied metabolic coverage, but with minimal use of internal standards (seven). The few reported LOD values were 540 nM, 10 nM and 30 nM for serine, phenylalanine and succinic acid, respectively, compared to 23.4 nM, 3.7 nM and 21.7 nM detected using DmPABr labelling (which minimises internal standard cost by applying ICD). Luo, Li [45] used dansyl-labelling derivatization prior

to nanoLC-MS, and detected 1620 ± 148 metabolite peak pairs from the amine/phenome submetabolome. This method also uses the chemical isotope labelling approach, creating internal standards for each metabolite for qualitative investigation, unlike the use in our work that allows quantitative analysis.

Conclusion

The presented work demonstrates an approach for sensitive metabolomics analysis of a low-cell number sample. Chemical derivatization by DmPABr, followed by a LC-MS/MS targeted analysis, allowed absolute quantification of 37 metabolites in a diluted extract of 1×10^4 HepG2 cells (equivalent of 10 cells on column), 27 metabolites in a diluted extract of 5×10^3 HepG2 cells (equivalent of 5 cells on column), 18 metabolites in a diluted extract of 1×10^3 HepG2 cells (equivalent of 1 cell on column) and 12 metabolites in a diluted extract of 250 HepG2 cells (an equivalent of 0.25 cells on column). The method was evaluated using chemically diverse metabolites of high biological importance that were already implicated in several health conditions. Owing to the ability of the DmPABr reagent to label a broad selection of metabolites, the method can be further expanded to a wider selection of metabolites, matrices and applications, and further optimized for greater sensitivity. This aligns with the growing need for sensitive quantification of material-limited samples, and can be successfully achieved by combining with micro/nano-LC or CE coupled to nanoESI-MS/MS.

Acknowledgements

The author expresses thanks to Dr. Wei Zhang at Leiden University for culturing and providing the HepG2 cells. This project was supported by the SysMedPD project, which has received funding from the European Union's Horizon 2020 research and innovation programme under grant agreement no, 668738.

References

1. Thompson Legault J, Strittmatter L, Tardif J, et al. A Metabolic Signature of Mitochondrial Dysfunction Revealed through a Monogenic Form of Leigh Syndrome. *Cell Rep.* 2015;13(5):981-989.
2. Karu N, Wilson R, Hamede R, et al. Discovery of Biomarkers for Tasmanian Devil Cancer (DFTD) by Metabolic Profiling of Serum. *J Proteome Res.* 2016;15(10):3827-3840.
3. Huberty M, Martis B, Van Kampen J, et al. Soil Inoculation Alters Leaf Metabolic Profiles in Genetically Identical Plants. *Journal of Chemical Ecology.* 2020:1-11.
4. Jozefczuk S, Klie S, Catchpole G, et al. Metabolomic and transcriptomic stress response of Escherichia coli. *Molecular systems biology.* 2010;6(1):364.
5. Madsen R, Lundstedt T, Trygg J. Chemometrics in metabolomics—a review in human disease diagnosis. *Analytica chimica acta.* 2010;659(1-2):23-33.
6. Shah SH, Kraus WE, Newgard CB. Metabolomic profiling for the identification of novel biomarkers and mechanisms related to common cardiovascular diseases: form and function. *Circulation.* 2012;126(9):1110-1120.
7. Tatar Z, Migne C, Petera M, et al. Variations in the metabolome in response to disease activity of rheumatoid arthritis. *BMC musculoskeletal disorders.* 2016;17(1):353.
8. Van Esbroeck AC, Janssen AP, Cognetta AB, et al. Activity-based protein profiling reveals off-target proteins of the FAAH inhibitor BIA 10-2474. *Science.* 2017;356(6342):1084-1087.
9. Hadrévi J, Ghafouri B, Sjörs A, et al. Comparative metabolomics of muscle interstitium fluid in human trapezius myalgia: an in vivo microdialysis study. *European journal of applied physiology.* 2013;113(12):2977-2989.
10. Trushina E, Dutta T, Persson X-MT, Mielke MM, Petersen RC. Identification of altered metabolic pathways in plasma and CSF in mild cognitive impairment and Alzheimer's disease using metabolomics. *PLoS One.* 2013;8(5):e63644.

11. Moreno EL, Hachi S, Hemmer K, et al. Differentiation of neuroepithelial stem cells into functional dopaminergic neurons in 3D microfluidic cell culture. *Lab Chip.* 2015;15(11):2419-2428.
12. Choi WT, Tosun M, Jeong H-H, et al. Metabolomics of mammalian brain reveals regional differences. *BMC Systems Biology.* 2018;12(8):127.
13. Taylor RM, Miller PR, Ebrahimi P, Polsky R, Baca JT. Minimally-invasive, microneedle-array extraction of interstitial fluid for comprehensive biomedical applications: transcriptomics, proteomics, metabolomics, exosome research, and biomarker identification. *Laboratory animals.* 2018;52(5):526-530.
14. Wevers NR, Van Vught R, Wilschut KJ, et al. High-throughput compound evaluation on 3D networks of neurons and glia in a microfluidic platform. *Sci Rep.* 2016;6(1):1-10.
15. Beaurivage C, Naumovska E, Chang YX, et al. Development of a gut-on-a-chip model for high throughput disease modeling and drug discovery. *International Journal of Molecular Sciences.* 2019;20(22):5661.
16. Kane KI, Moreno EL, Hachi S, et al. Automated microfluidic cell culture of stem cell derived dopaminergic neurons. *Sci Rep.* 2019;9(1):1-12.
17. Higashi T, Ogawa S. Isotope-coded ESI-enhancing derivatization reagents for differential analysis, quantification and profiling of metabolites in biological samples by LC/MS: A review. *J Pharm Biomed Anal.* 2016;130:181-193.
18. Ramautar R, Somsen GW, de Jong GJ. CE-MS for metabolomics: Developments and applications in the period 2016–2018. *Electrophoresis.* 2019;40(1):165-179.
19. Nassar AF, Wu T, Nassar SF, Wisnewski AV. UPLC–MS for metabolomics: a giant step forward in support of pharmaceutical research. *Drug discovery today.* 2017;22(2):463-470.
20. Yi X, Leung EKY, Bridgman R, Koo S, Yeo K-TJ. High-sensitivity micro LC-MS/MS assay for serum estradiol without derivatization. *Journal of Applied Laboratory Medicine.* 2016;1(1):14-24.
21. Kantae V, Ogino S, Noga M, et al. Quantitative profiling of endocannabinoids and related N-acylethanolamines in human CSF using nano LC-MS/MS. *J Lipid Res.* 2017;58(3):615-624.

22. Zhang W, Guled F, Hankemeier T, Ramautar R. Utility of sheathless capillary electrophoresis-mass spectrometry for metabolic profiling of limited sample amounts. *Journal of Chromatography B.* 2019;1105:10-14.
23. Hirayama A, Tomita M, Soga T. Sheathless capillary electrophoresis-mass spectrometry with a high-sensitivity porous sprayer for cationic metabolome analysis. *Analyst.* 2012;137(21):5026-5033.
24. Chetwynd AJ, David A. A review of nanoscale LC-ESI for metabolomics and its potential to enhance the metabolome coverage. *Talanta.* 2018;182:380-390.
25. Chetwynd AJ, David A, Hill EM, Abdul-Sada A. Evaluation of analytical performance and reliability of direct nanoLC-nanoESI-high resolution mass spectrometry for profiling the (xeno) metabolome. *Journal of Mass Spectrometry.* 2014;49(10):1063-1069.
26. Maciel EVS, de Toffoli AL, Sobieski E, Nazário CED, Lanças FM. Miniaturized liquid chromatography focusing on analytical columns and mass spectrometry: A review. *Analytica Chimica Acta.* 2020;1103:11-31.
27. Villas-Bôas SG, Smart KF, Sivakumaran S, Lane GA. Alkylation or silylation for analysis of amino and non-amino organic acids by GC-MS? *Metabolites.* 2011;1(1):3-20.
28. Wong JM, Malec PA, Mabrouk OS, Ro J, Dus M, Kennedy RT. Benzoyl chloride derivatization with liquid chromatography-mass spectrometry for targeted metabolomics of neurochemicals in biological samples. *J Chromatogr A.* 2016;1446:78-90.
29. Guo K, Li L. Differential 12C-/13C-isotope dansylation labeling and fast liquid chromatography/mass spectrometry for absolute and relative quantification of the metabolome. *Anal Chem.* 2009;81(10):3919-3932.
30. Guo K, Li L. High-Performance Isotope Labeling for Profiling Carboxylic Acid-Containing Metabolites in Biofluids by Mass Spectrometry. *Analytical Chemistry.* 2010;82(21):8789-8793.
31. Guo H, Jiao Y, Wang X, Lu T, Zhang Z, Xu F. Twins labeling-liquid chromatography/mass spectrometry based metabolomics for absolute quantification of tryptophan and its key metabolites. *J Chromatogr A.* 2017;1504:83-90.

32. Lkhagva A, Shen C-C, Leung Y-S, Tai H-C. Comparative study of five different amine-derivatization methods for metabolite analyses by liquid chromatography-tandem mass spectrometry. *Journal of Chromatography A.* 2020;1610:460536.
33. Song P, Mabrouk OS, Hershey ND, Kennedy RT. In vivo neurochemical monitoring using benzoyl chloride derivatization and liquid chromatography-mass spectrometry. *Anal Chem.* 2012;84(1):412-419.
34. Willacey CCW, Naaktgeboren M, Lucumi Moreno E, et al. LC–MS/MS analysis of the central energy and carbon metabolites in biological samples following derivatization by dimethylaminophenacyl bromide. *Journal of Chromatography A.* 2019:460413.
35. Gunda V, Yu F, Singh PK. Validation of Metabolic Alterations in Microscale Cell Culture Lysates Using Hydrophilic Interaction Liquid Chromatography (HILIC)-Tandem Mass Spectrometry-Based Metabolomics. *PLoS One.* 2016;11(4):e0154416.
36. Prinsen H, Schiebergen-Bronkhorst BGM, Roeleveld MW, et al. Rapid quantification of underivatized amino acids in plasma by hydrophilic interaction liquid chromatography (HILIC) coupled with tandem mass-spectrometry. *Journal of inherited metabolic disease.* 2016;39(5):651-660.
37. Heaton JC, McCalley DV. Some factors that can lead to poor peak shape in hydrophilic interaction chromatography, and possibilities for their remediation. *Journal of Chromatography A.* 2016;1427:37-44.
38. Ibáñez AB, Bauer S. Analytical method for the determination of organic acids in dilute acid pretreated biomass hydrolysate by liquid chromatography-time-of-flight mass spectrometry. *Biotechnol Biofuels.* 2014;7(1):145-145.
39. Peng M, Liu L, Jiang M, et al. Measurement of free carnitine and acylcarnitines in plasma by HILIC-ESI-MS/MS without derivatization. *Journal of Chromatography B.* 2013;932:12-18.
40. Mardinoglu A, Shoaie S, Bergentall M, et al. The gut microbiota modulates host amino acid and glutathione metabolism in mice. *Mol Syst Biol.* 2015;11(10):834.
41. Annesley TM. Ion suppression in mass spectrometry. *Clinical chemistry.* 2003;49(7):1041-1044.

42. Quinete N, Bertram J, Reska M, Lang J, Kraus T. Highly selective and automated online SPE LC–MS3 method for determination of cortisol and cortisone in human hair as biomarker for stress related diseases. *Talanta.* 2015;134:310-316.
43. Liu Q, Cai J, Nichols RG, et al. A Quantitative HILIC–MS/MS Assay of the Metabolic Response of Huh-7 Cells Exposed to 2, 3, 7, 8-Tetrachlorodibenzo-p-Dioxin. *Metabolites.* 2019;9(6):118.
44. Danielsson AP, Moritz T, Mulder H, Spégel P. Development and optimization of a metabolomic method for analysis of adherent cell cultures. *Analytical biochemistry.* 2010;404(1):30-39.
45. Luo X, Li L. Metabolomics of Small Numbers of Cells: Metabolomic Profiling of 100, 1000, and 10000 Human Breast Cancer Cells. *Analytical Chemistry.* 2017;89(21):11664-11671.

Supplementary information

Table S1. List of the ChEBI identifiers for the metabolites investigated in this methodology

Metabolite	ChEBI ID	Metabolite	ChEBI ID
Alanine	16977	N-acetylthreonine	45826
Arginine	16467	N-acetyltryptophan	70976
Asparagine	17196	N-acetyltyrosine	21563
Aspartic acid	17053	N-acetylvaline	21565
Cysteine	17561	α-Ketoglutaric acid	30915
Glutamine	18050	Citrates	30769/30887
Glutamic acid	16015	Fumaric acid	18012
Glycine	15428	Lactic acid	28358
Histidine	15971	Malic acid	6650
Isoleucine	17191	Oxaloacetic acid	30744
Leucine	15603	Pyruvic acid	32816
Lysine	18019	Succinic acid	15741
Methionine	16643	Acetylcarnitine	57589
Phenylalanine	17295	Decanoylcarnitine	68830
Proline	17203	Hexanoylcarnitine	70749
Serine	17115	Lauroylcarnitine	77086
Threonine	16857	Myristoylcarnitine	84634
Tryptophan	16828	Octanoylcarnitine	73039
Tyrosine	17895	Palmitoylcarnitine	73067
Valine	16414	Propionylcarnitine	28867
N-acetylalanine	40992	Stearoylcarnitine	73074
N-acetylarginine	40521	Decanoic acid	30813
N-acetylaspartic acid	21547	Octanoic acid	28837
N-acetylglutamine	21553	Dodecanoic acid	30805
N-acetylglycine	40410	Undecanoic Acid	32368
N-acetylmethionine	21557	Creatinine	16737

Table S2. Retention time and MRM parameters for the measurement of the metabolites covered within this method. The ICD generated internal standards are noted by the addition of –IS to the metabolite name.

Metabolite	Precusor	Product	RT	CE
Alanine	573.2	366.2	5.23	20
Arginine	658.2	319.2	4.71	35
Asparagine	616.2	339.2	4.94	30
Aspartic acid	778.2	392.2	5.6	30
Cysteine	766.2	134.1	5.6	25
Glutamine	630.2	340.2	4.91	20
Glutamic acid	792.2	585.2	5.68	35
Glycine	559.2	134.1	5.2	30
Histidine	400.83	134.1	4.98	40
Isoleucine	615.2	408.2	5.83	30
Leucine	615.2	408.2	5.87	30
Lysine	476.6	134.1	5.5	30
Methionine	633.2	426.2	5.62	25
Phenylalanine	649.2	442.2	5.77	30
Proline	438.1	289.1	3.8	25
Serine	589.2	408.2	5.15	25
Threonine	603.2	422.2	5.31	25
Tryptophan	688.2	340.2	5.56	30
Tyrosine	665.2	458.2	5.28	30
Valine	601.2	394.2	5.75	30
N-acetylalanine	293.13	180	2.99	15
N-acetylglycine	279.11	180	2.74	15
N-acetylvaline	321.19	180	3.68	15
N-acetyltryptophan	408.27	180	4.07	15
N-acetyltyrosine	385.23	180	3.41	15
N-acetylaspragine	498.14	180	4.26	30
N-acetylarginine	378.24	180	2.35	30
N-acetylthreonine	323.16	180	2.82	20
N-acetylmethionine	353.25	180	3.65	15

Metabolite	Precusor	Product	RT	CE
N-acetylglutamine	350.18	84	2.51	25
Pyruvic acid	250.05	134	3.55	30
α-Ketoglutaric acid	469.2	134	4.79	30
Malic acid	457.07	134	4.31	35
Lactic acid	252.07	180	2.99	30
Citric/isocitric acid	676.101	180	5.1	20
Succinic acid	441.07	134	4.68	20
Fumaric acid	439.06	134	3.8	30
Oxaloacetic acid	455.06	134	3.46	35
C2:0-carnitine	365.11	134	2.64	20
C8:0-carnitine	449.04	134	4.6	35
C3:0-carnitine	379.21	134	2.94	35
C16:0-carnitine	561.6	134	6.26	35
C18:0-carnitine	589.7	134	6.55	35
C14:0-carnitine	533.6	134	5.92	35
C6:0-carnitine	421.4	134	3.95	35
C10:0-carnitine	477.5	134	5.11	35
C12:0-carnitine	505.5	134	5.54	35
Octanoic acid	306.21	180	5.65	20
Decanoic acid	334.26	180	6.08	20
Dodecanoic acid	362.32	180	6.44	20
Undecanoic acid	348.29	180	6.27	20
Creatinine	275.12	134.1	2.12	40
IS-Alanine	579.2	370.2	5.23	25
IS-Arginine	664.2	321.2	4.71	35
IS-Asparagine	622.2	343.2	4.94	30
IS-Aspartic acid	786.2	396.2	5.6	30
IS-Cysteine	774.2	136.1	5.6	25
IS-Glutamine	636.2	344.2	4.91	30
IS-Glutamic acid	800.2	591.2	5.68	35
IS-Glycine	565.2	136.1	5.2	30
IS-Isoleucine	621.2	412.2	5.83	30
IS-Leucine	621.2	412.2	5.87	30

Metabolite	Precusor	Product	RT	CE
IS-Lysine	481.6	136.1	5.5	30
IS-Methionine	639.2	430.2	5.62	25
IS-Phenylalanine	655.2	446.2	5.77	30
IS-Proline	442.1	291.1	3.8	25
IS-Serine	595.5	412.2	5.15	25
IS-Threonine	609.2	426.2	5.31	25
IS-Tryptophan	694.2	344.2	5.56	30
IS-Tyrosine	671.2	462.2	5.28	30
IS-Valine	607.2	398.2	5.75	30
IS-Histidine	645.2	136.1	4.98	40
IS-N-acetylalanine	295.1	182	2.99	15
IS-N-acetylglycne	281.1	182	2.74	15
IS-N-acetylvaline	323.2	182	3.68	15
IS-N-acetyltryptophan	410.3	182	4.07	15
IS-N-acetyltyrosine	387.2	182	3.41	15
IS-N-acetylaspartic acid	502.1	182	4.26	30
IS-N-acetylarginine	380.2	182	2.35	30
IS-N-acetylthreonine	325.2	182	2.82	20
IS-N-acetylmethionine	355.3	182	3.65	15
IS-N-acetylglutamine	352.2	84	2.54	25
IS-Pyruvic acid	252.1	136	3.55	30
IS-Alpha-Ketoglutaric acid	473.2	136	4.79	30
IS-Malic acid	461.1	136	4.31	35
IS-Lactic acid	254.1	182	2.99	30
IS-Citric/Isocitric acid	682.1	182	5.1	40
IS-Succinic acid	445.1	136	4.68	30
IS-Fumaric acid	443.1	136	3.8	30
IS-Oxaloacetic acid	459.1	136	3.46	35
IS-C2:0-carnitine	367.1	136	2.64	35
IS-C8:0-carnitine	451	136	4.6	35
IS-C3:0-carnitine	381.2	136	2.94	35
IS-Octanoic acid	308.2	182	5.56	20
IS-Decanoic acid	336.2	182	6.08	20

Metabolite	Precusor	Product	RT	CE
IS-Dodecanoic acid	364.3	182	6.44	20
IS-Undecanoic acid	350.3	182	6.27	20
IS-Creatinine	277.1	136	2.12	40
IS-C16:0-carnitine	563.6	136	6.26	35
IS-C18:0-carnitine	592.7	136	6.55	35
IS-C14:0-carnitine	535.6	136	5.92	35
IS-C6:0-carnitine	423.4	136	3.95	35
IS-C10:0-carnitine	479.5	136	5.11	35
IS-C12:0-carnitine	507.5	136	5.54	35

Table S3. Calibration stock concentration of the metabolites measured within this method

Metabolite	Stock concentration (µM)	Metabolite	Stock concentration (µM)
Alanine	594.29	**N-acetylthreonine**	19.71
Arginine	74.29	**N-acetyltryptophan**	3.49
Asparagine	267.43	**N-acetyltyrosine**	1.79
Aspartic acid	148.57	**N-acetylvaline**	8.76
Cysteine	891.43	**α-Ketoglutaric acid**	148.57
Glutamine	891.43	**Citrates**	3714.29
Glutamic acid	59.43	**Fumaric acid**	14.86
Glycine	4457.14	**Lactic acid**	297.14
Histidine	1782.86	**Malic acid**	29.71
Isoleucine	59.43	**Oxaloacetic acid**	29.71
Leucine	89.14	**Pyruvic acid**	32.4
Lysine	445.71	**Succinic acid**	118.86
Methionine	29.71	**Acetylcarnitine**	59.43
Phenylalanine	178.29	**Decanoylcarnitine**	29.71
Proline	14.86	**Hexanoylcarnitine**	14.29
Serine	891.43	**Lauroylcarnitine**	14.29
Threonine	356.57	**Myristoylcarnitine**	14.29
Tryptophan	178.29	**Octanoylcarnitine**	1.49
Tyrosine	237.71	**Palmitoylcarnitine**	14.29
Valine	118.86	**Propionylcarnitine**	14.29
N-acetylalanine	19.71	**Stearoylcarnitine**	14.29
N-acetylarginine	17.11	**Decanoic acid**	29.71
N-acetylaspartic acid	47.56	**Octanoic acid**	29.71
N-acetylglutamine	32.4	**Dodecanoic acid**	0.89
N-acetylglycine	9.3	**Undecanoic Acid**	2.97
N-acetylmethionine	92.43	**Creatinine**	1857.14

Fig S1. LC-MS/MS Total Ion Count chromatograms of a range of dilutions of HepG2 cells, derivatized by DmPABr. Top trace, 1×10⁴ cells; middle trace, 5×10³ cells; bottom trace, 2.5×10³ cells.

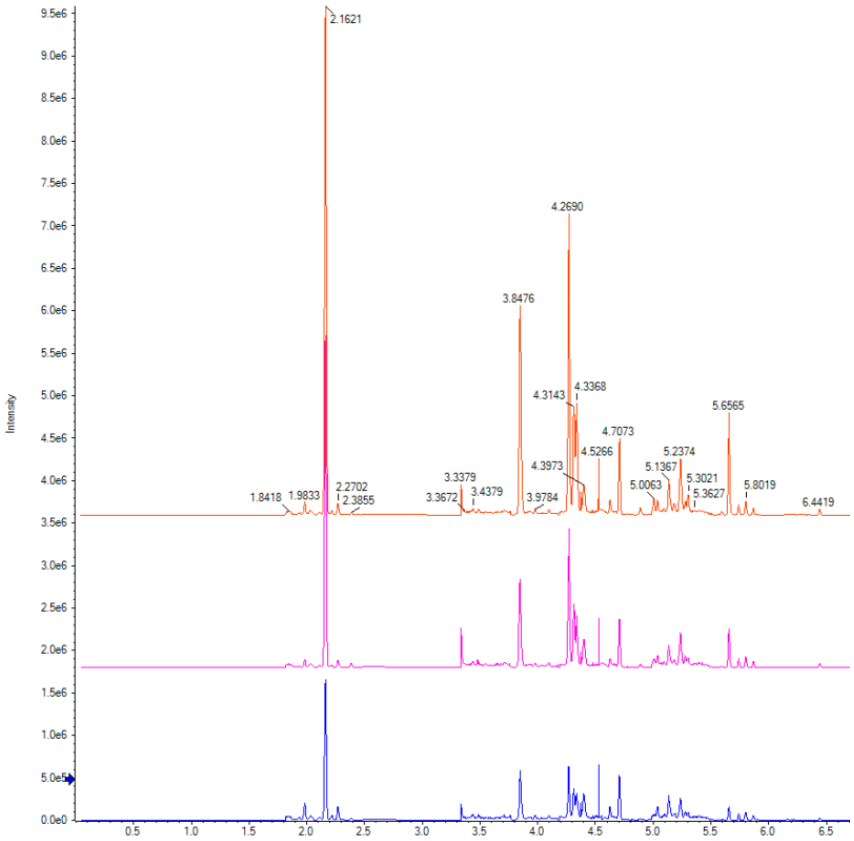

Fig S2. Extracted ion chromatogram from a neat standard solution showing the co-elution of the analytes (blue) with the internal standard (pink) using the isotope-coded derivatization approach. A) alanine; B) myristoylcarnitine; C) N-acetylated aspartic acid; D) isoleucine and leucine (left to right).

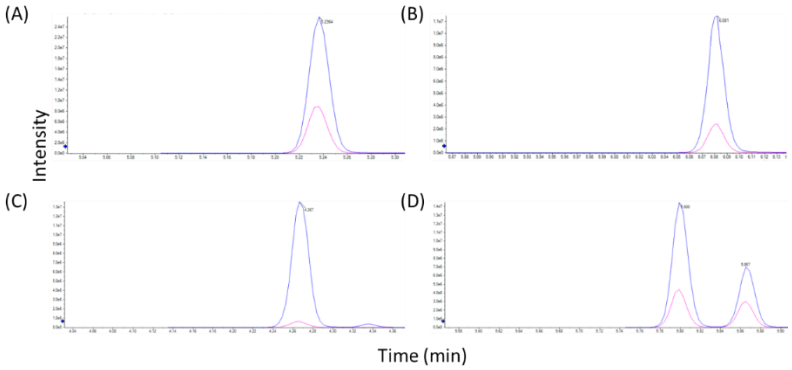

Table S4. Summary of the metabolites cell coverage range and linearity of the cell concentrations across a range of dilution

Metabolite	Cell number range	R^2	Metabolite	Cell number range	R^2
Alanine	250-1e5	0.985	**N-acetylthreonine**	1e4-1e5	0.999
Arginine	1e3-1e5	0.991	**N-acetyltryptophan**	5e4-1e5	N/A
Asparagine	1e4-1e5	0.99	**N-acetyltyrosine**	1e4-1e5	0.99
Aspartic acid	1e3-1e5	0.998	**N-acetylvaline**	2.5e4-1e5	0.981
Cysteine	2.5e4-1e5	0.984	**α-Ketoglutaric acid**	2.5e4-1e5	0.982
Glutamine	1e3-1e5	0.978	**Citrates**	1e4-1e5	0.995
Glutamic acid	250-1e5	0.99	**Fumaric acid**	250-1e5	0.999
Glycine	250-1e5	0.985	**Lactic acid**	2.5e3-1e5	0.995
Histidine	1e5	N/A	**Malic acid**	250-1e5	1
Isoleucine	1e3-1e5	0.978	**Oxaloacetic acid**	5e3-1e5	0.989
Leucine	500-1e5	0.975	**Pyruvic acid**	250-1e5	0.985
Lysine	5e3-1e5	0.976	**Succinic acid**	2.5e3-1e5	0.995
Methionine	5e3-1e5	0.979	**Acetylcarnitine**	5e4-1e5	N/A
Phenylalanine	5e3-1e5	0.976	**Decanoylcarnitine**	5e3-1e5	0.997
Proline	250-1e5	1	**Hexanoylcarnitine**	2.5e4-1e5	0.992
Serine	250-1e5	0.986	**Lauroylcarnitine**	5e4-1e5	N/A
Threonine	250-1e5	0.982	**Myristoylcarnitine**	1e4-1e5	0.998
Tryptophan	1e4-1e5	0.979	**Octanoylcarnitine**	2.5e4-1e5	0.981
Tyrosine	1e3-1e5	0.98	**Palmitoylcarnitine**	2.5e3-1e5	0.997
Valine	250-1e5	0.978	**Propionylcarnitine**	2.5e4-1e5	0.986
N-acetylalanine	2.5e4-1e5	0.997	**Stearoylcarnitine**	2.5e3-1e5	0.997
N-acetylarginine	5e4-1e5	N/A	**Decanoic acid**	1e4-1e5	0.987
N-acetylaspartic acid	250-1e5	0.998	**Octanoic acid**	2.5e4-1e5	0.986
N-acetylglutamine	5e4-1e5	1	**Dodecanoic acid**	1e4-1e5	0.992
N-acetylglycine	1e4-1e5	0.973	**Undecanoic Acid**	2.5e4-1e5	0.999
N-acetylmethionine	1e4-1e5	0.997	**Creatinine**	250-1e5	0.997

Table S5. Summary of the metabolite asymmetry factors from the measurement of neat calibration standard at the midpoint concentration.

Metabolite	Asymmetry factor	Metabolite	Asymmetry factor
Alanine	1.11	**N-acetylthreonine**	1.17
Arginine	1.05	**N-acetyltryptophan**	0.86
Asparagine	0.97	**N-acetyltyrosine**	1.17
Aspartic acid	1.22	**N-acetylvaline**	1.08
Cysteine	0.90	**α-Ketoglutaric acid**	0.96
Glutamine	1.15	**Citrates**	1.92
Glutamic acid	1.31	**Fumaric acid**	1.59
Glycine	1.14	**Lactic acid**	0.98
Histidine	1.19	**Malic acid**	1.14
Isoleucine	1.04	**Oxaloacetic acid**	1.28
Leucine	0.97	**Pyruvic acid**	0.97
Lysine	1.01	**Succinic acid**	1.15
Methionine	1.01	**Acetylcarnitine**	1.11
Phenylalanine	0.91	**Decanoylcarnitine**	1.25
Proline	1.14	**Hexanoylcarnitine**	0.98
Serine	1.89	**Lauroylcarnitine**	0.88
Threonine	0.93	**Myristoylcarnitine**	0.99
Tryptophan	1.19	**Octanoylcarnitine**	1.27
Tyrosine	1.31	**Palmitoylcarnitine**	1.06
Valine	1.01	**Propionylcarnitine**	1.09
N-acetylalanine	1.05	**Stearoylcarnitine**	1.10
N-acetylarginine	1.04	**Decanoic acid**	1.18
N-acetylaspartic acid	1.15	**Octanoic acid**	1.03
N-acetylglutamine	1.12	**Dodecanoic acid**	0.97
N-acetylglycine	1.26	**Undecanoic Acid**	0.86
N-acetylmethionine	1.08	**Creatinine**	0.92

3